The Electronic Structure of ScAl+. Ground and Low-Lying Excited States

Demeter Tzeli and Aristides Mavridis*

Laboratory of Physical Chemistry, Department of Chemistry, National and Kapodistrian University of Athens, P.O. Box 64 004, 157 10 Zografou, Athens, Greece

Using semiquantitative basis sets and ab initio multireference methods, we have investigated the electronic structure of scandium aluminide cation, ScAl+. In addition to the ground state ($X^2\Delta$), we have constructed potential energy curves for 20 more states spanning an energy range of no more than 1.5 eV. The first three states, $X^2\Delta$, $1^2\Pi$, and $2^2\Sigma^+$, are practically degenerate within the accuracy of our calculations. They have similar binding modes and a binding energy of about 30 kcal/mol with respect to their adiabatic fragments $Sc(^2D) + Al^+(^1S)$. The rest of the states correlate to $Sc^+(^3D$ or $^3F) + Al(^2P)$. For all states we report bond lengths, dissociation energies, harmonic frequencies, Mulliken charges, and energy gaps.

1. Introduction

The 3d transition metal aluminides form an important class of high-temperature materials with some of them being candidates for permanent magnets.[1] A systematic study through electronic spectroscopy of 3d transition metal aluminides but with the exception of the ScAl species is given in ref 2, while for ScAl alloys there are some limited experimental data on enthalpies of formation.[3–5] Given the increasing importance of these materials, our interest in the isovalent metal borides, M–B+ (M = Sc, Ti, V, Cr),[6] and the complete lack of experimental and/or theoretical information on ScAl+, we have decided to probe the electronic structure of this diatomic cation by ab initio quantum methods.

In the present work the electronic structure of ScAl+ is investigated via complete active space SCF (CASSCF) and multireference configuration interaction (MRCI = CASSCF + single + double replacements = CASSCF +1 + 2) methods. In addition to the ground state ($X^2\Delta$, vide infra), 20 low-lying excited states have been also examined: 10 doublets $\{2^2\Sigma^+, 11^2\Sigma^+, 7^2\Sigma^-, 20^2\Sigma^-, 1^2\Pi, 9^2\Pi, 13^2\Pi, 8^2\Delta, 14^2\Delta, 12^2\Phi\}$ and 10 quartets $\{15^4\Sigma^+, 19^4\Sigma^+, 3^4\Sigma^-, 18^4\Sigma^-, 4^4\Pi, 10^4\Pi, 17^4\Pi, 6^4\Delta, 16^4\Delta, 5^4\Phi\}$. One of the interesting aspects of the present report is the comparable ionization potentials of Sc and Al atoms, 6.56 and 5.98 eV, respectively;[7] as a result the ground ($X^2\Delta$) and the first two excited states ($1^2\Pi$, $2^2\Sigma^+$) of ScAl+ correlate to $Sc(^2D) + Al^+(^1S)$, while the rest of the states correlate to $Sc^+(^3D$ or $^3F) + Al(^2P)$.

For all 21 states examined we report full potential energy curves (PEC), binding energies (D_e), bond distances (R_e), harmonic frequencies (ω_e), Mulliken populations, and energy gaps (T_e), while emphasis has been given in deciphering the bonding mechanism(s) with the help of simple valence bond Lewis (vbL) diagrams.

2. Methods

For the Sc atom the ANO basis set of Bauschlicher[8] (21s16p9d6f4g) has been used but with the functions of *g* angular momentum removed. For the Al atom, the cc-pVTZ (15s9p2d1f) basis set of Dunning[9] was employed. Both sets were generally contracted to $[(7s6p4d3f)_{Sc}/(5s4p2d1f)_{Al}]$, numbering 100 spherical Gaussians.

As already indicated, the complete active space SCF (CASSCF) methodology was employed to describe the reference space, followed by single and double configuration interaction out of the CASSCF space (CASSCF + 1 + 2 = MRCI). Five "valence" (active) electrons were distributed to 10 orbital functions for the quartets (one 4s and five 3d's on Sc + one 3s and three 3p's on Al), and to 11 orbitals (+ one $4p_z$) for the doublets. The additional $4p_z$ orbital function was deemed necessary for the $X^2\Delta$, $1^2\Pi$, and $2^2\Sigma^+$ states correlating to Sc + Al+, but for reasons of uniformity the 11 orbital space was maintained in all doublets. Depending on the number of orbitals and the symmetry of the state, our reference spaces range from 432 to 1354 configuration functions (CF), with corresponding CI numbers ranging from 431 318 to 871 611 CFs at the MRCI level. By applying the internal contraction (icMRCI) technique,[10] the number of CFs is reduced by about half. All calculations were done under C_{2v} symmetry constraints; however care was exercised for the CASSCF wave functions to display correct axial angular momentum symmetry, i.e., $|\Lambda| = 0, 1, 2,$ and 3 or $\Sigma^\pm$, Π, Δ, and Φ, respectively. This means that Δ states are linear combinations of A_1 and A_2 symmetries, Π and Φ states are combinations of B_1 and B_2 symmetries, and Σ^+ and Σ^- states correspond to the A_1 and A_2 symmetry species, respectively. MRCI wave functions do not display in general pure axial symmetry, being calculated as A_1 or A_2 and B_1 or B_2. With the exception of the $X^2\Delta$, $1^2\Pi$, $2^2\Sigma^+$, and $3^4\Sigma^-$ states, the state average (SA) approach[11,12] was used for the computation of all other states. Numerical experiments performed for some of the lowest states with and without the SA method and with and without internal contraction showed absolute energy losses of no more than 2 mhartrees collectively. Finally, the size nonextensivity errors of our SA–icMRCI wave functions are less than 1 mhartree.

All calculations were performed with the MOLPRO suite of codes,[13] while some of the lower states were also checked with the COLUMBUS code.[14]

3. Description of the Atoms

Absolute energies of $Sc(^2D)$, $Sc^+(^3D,^1D,^3F)$, and $Al(^2P)$, $Al^+(^1S)$, atomic energy separations, and ionization potentials are listed in Table 1. The SCF and CASSCF calculations were done

TABLE 1: Total Energies (hartrees) of Sc(^{2}D), Sc$^+$(^{3}D,^{1}D,^{3}F), Al(^{2}P), and Al$^+$(^{1}S), Atomic Energy Separations (eV) of Sc$^+$, and Ionization Potential (IP, eV) of Sc and Al

| | Sc | | Al | |
method	^{2}D	IP	^{2}P	IP
SCF[a]	−759.735 546	5.353	−241.875 030	5.487
CISD	−759.776 234	6.330	−241.929 677	5.899
CASSCF[a]	−759.736 719	5.385	−241.893 139	5.980
MRCI[b]	−759.777 063	6.352	−241.931 231	5.941
FCI[c]	−759.778 012	6.378	−241.931 618	5.952
expt[d]		6.56		5.984

| | Sc$^+$ | | | | | Al$^+$ |
method	^{3}D	^{1}D	3F	^{1}D ← ^{3}D	^{3}F ← ^{3}D	^{1}S
SCF[a]	−759.538 831	−759.520 837	−759.509 640	0.490	0.794	−241.673 376
CISD	−759.543 617	−759.534 067	−759.517 701	0.260	0.705	−241.712 900
expt[d]				0.302	0.596	

[a] Spherically averaged SCF, CASSCF. [b] Internally contracted MRCI. [c] Full (valence) CI, i.e., SCF+1+2+3. [d] Reference 7.

under spherically averaged restrictions; for the neutrals Sc and Al full (valence) configuration interaction calculations (FCI = SCF +1 +2 +3) are also reported out of the spherically averaged SCF reference functions. Notice the good agreement between theory and experiment of Al IP, its slight improvement going to FCI results, the not so good agreement between experiment and theory of the Sc IP even at the FCI level (smaller by 0.182 eV = 4.20 kcal/mol), and the difference of +0.109 eV of the Sc ^{3}F ← ^{3}D energy splitting. Notwithstanding the foregoing discrepancies, the overall performance of the chosen basis set is judged as adequate for our purpose, the observed differences between experiment and theory being rather caused by differential correlation effects.[15]

4. Results and Discussion

Table 2 presents total energies (E), bond lengths (R_e), dissociation energies (D_e) with respect to the adiabatic products, harmonic frequencies (ω_e), Mulliken charges (q_{Sc}), and energy gaps (T_e) at the CASSCF, ic-MRCI/ANO(Sc)-cc-pVTZ (Al) level of theory, of 21 states with symmetries $^{2,4}\Sigma^\pm$, $^{2,4}\Pi$, $^{2,4}\Delta$, and $^{2,4}\Phi$. Also, for indicative reasons, total energies and related quantities are presented at the ic-MRCI+Q (ic-MRCI + multireference Davidson correction[16]). Figure 1 shows all calculated potential energy curves (PEC), while Figure 2 depicts relative energies of all states studied, along with a similar diagram of the isovalent ScB^{+} [6a] species for reasons of comparison. Each state has been tagged with a serial number in front of the symmetry symbol indicating its absolute energy order with respect to the ground (X) state. Notice that we cover a total energy range of no more than 1.5 eV, while some of the states are practically degenerate within the accuracy of our methods.

In the ensuing discussion we refer to the first three states "naturally" grouped under symmetries Δ, Π, and Σ, then we discuss the $3^4\Sigma^-$ state, the rest of the doublets follow, and finally we discuss the remaining higher nine quartets.

4.1. X$^2\Delta$, 1$^2\Pi$, and 2$^2\Sigma^+$ States. No state average (SA) was employed in the calculation of the above states, which are tracing their ancestry to $|$Sc, ^{2}D; $M = \pm2, \pm1, 0\rangle \otimes |Al^+$, ^{1}S; $M = 0\rangle$. At the equilibrium the leading CASSCF configurations are

$$|\text{X}^2\Delta\rangle \sim 0.91[1/\sqrt{2}(|1\sigma^2 2\sigma^2 1\delta_+{}^1\rangle + |1\sigma^2 2\sigma^2 1\delta_-{}^1\rangle)]$$

$$|1^2\Pi\rangle \sim 0.92[1/\sqrt{2}(|1\sigma^2 2\sigma^2 1\pi_x{}^1\rangle + |1\sigma^2 2\sigma^2 1\pi_y{}^1\rangle)]$$
$$|2^2\Sigma^+\rangle \sim 0.92|1\sigma^2 2\sigma^2 3\sigma^1\rangle$$

with the following CASSCF atomic Mulliken populations, Sc/ Al. Obviously the Mulliken distributions are very similar for

$$\Delta: 4s^{1.28}3d_{z^2}^{0.06}3d_{x^2-y^2}^{0.50}3d_{xy}^{0.50}3d_{xz}^{0.01}3d_{yz}^{0.01}4p_x^{0.01}4p_y^{0.01}4p_z^{0.13}/$$
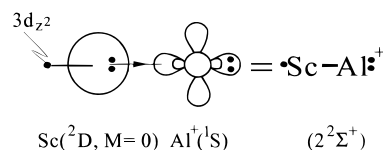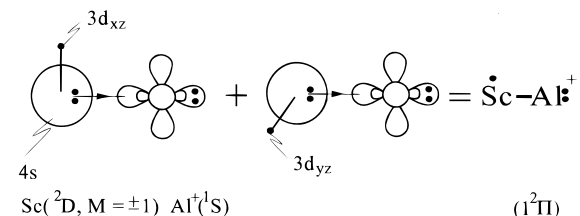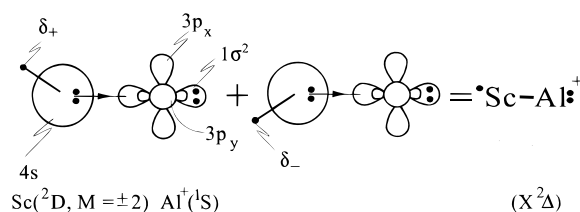$$3s^{1.82}3p_x^{0.05}3p_y^{0.05}3p_z^{0.53}$$

$$\Pi: \quad 4s^{1.34}3d_{z^2}^{0.05}3d_{xz}^{0.50}3d_{yz}^{050}4p_z^{0.12}/3s^{1.84}3p_x^{0.05}3p_y^{0.05}3p_z^{0.53}$$

$$\Sigma: \quad 4s^{1.32}3d_{z^2}^{1.03}4p_z^{0.10}/3s^{1.83}3p_x^{0.04}3p_y^{0.04}3p_z^{0.57}$$

all three states differing only in the symmetry-defining, "observer" electron, d$_\delta$, d$_\pi$, and d$_\sigma$, respectively.

All three states are practically degenerate (Figure 1, Table 2), with the X$^2\Delta$ being formally the ground state at the MRCI level. However, after applying the Davidson correction (+Q), the order between the X$^2\Delta$ and 1$^2\Pi$ states is reversed, and the latter is stabilized with respect to the former by 0.5 mhartree.

In accordance with the asymptotic products and the populations, the bonding mechanism of these three states can be clearly represented by the following valence bond Lewis (vbL) pictures:

$$\text{Sc}(^2\text{D, } M = \pm2) \quad \text{Al}^+(^1\text{S}) \qquad\qquad (\text{X }^2\Delta)$$

$$\text{Sc}(^2\text{D, } M = \pm1) \quad \text{Al}^+(^1\text{S}) \qquad\qquad (1^2\Pi)$$

$$\text{Sc}(^2\text{D, } M = 0) \quad \text{Al}^+(^1\text{S}) \qquad (2^2\Sigma^+)$$

We observe that in all the above three states the atoms are held together by a pure σ-bond of practically equal energy

TABLE 2: Absolute Energies E (hartrees), Bond Lengths R_e (Å), Binding Energies D_e (kcal/mol), Harmonic Frequencies ω_e (cm^{-1}), Total Number of Electrons on Sc (N_e^-), and Energy Differences T_e (kcal/mol), at CASSCF, MRCI,[a] and MRCI+Q[b] Level

state[c]	methods	E	R_e	D_e	ω_e	N_e^-	T_e
X²Δ(1)	CASSCF	−1001.518 79	3.415	25.5	160	20.51	0.0
	MRCI	−1001.540 99	3.382	31.1	168	20.50	0.0
	MRCI+Q	−1001.541 7	3.38	31			0.0
1²Π(1)	CASSCF	−1001.505 05	3.464	26.8	147	20.51	8.6
	MRCI	−1001.540 03	3.312	30.9	163	20.52	0.6
	MRCI+Q	−1001.542 2	3.30	31			−0.3
2²Σ⁺(1)	CASSCF	−1001.513 86	3.421	21.7	151	20.46	3.1
	MRCI	−1001.539 60	3.358	29.7	164	20.52	0.9
	MRCI+Q	−1001.540 4	3.35	30			0.8
3⁴Σ⁻(1)	CASSCF	−1001.485 55	2.754	21.0	253	20.49	20.9
	MRCI	−1001.527 44	2.755	32.6	257	20.41	8.5
	MRCI+Q	−1001.529 8	2.76	34			7
4⁴Π(1)	CASSCF	−1001.462 94	2.974	19.0	189	20.45	35.0
	MRCI	−1001.518 32	2.917	27.6	202	20.44	14.2
	MRCI+Q	−1001.522 3	2.92	30			12
5⁴Φ(1)	CASSCF	−1001.455 13	2.966	14.3	210	20.38	39.9
	MRCI	−1001.511 07	2.930	22.8	227	20.37	18.8
	MRCI+Q	−1001.515 2	2.94	24			17
6⁴Δ(1)	CASSCF	−1001.477 62	3.568	20.9	120	20.45	25.8
	MRCI	−1001.510 02	3.387	21.6	138	20.48	19.4
	MRCI+Q	−1001.511 8	3.37	22			19
7²Σ⁻(1)	CASSCF	−1001.456 86	2.702	14.9	276	20.42	38.9
	MRCI	−1001.507 13	2.726	20.3	253	20.42	21.2
	MRCI+Q	−1001.510 7	2.74	21			19
8²Δ(g)(2)	CASSCF	−1001.454 91	2.857	11.8	246	20.37	40.1
	MRCI	−1001.506 72	2.844	20.1	312	20.39	21.5
	MRCI+Q	−1001.510 5	2.85	21			20
9²Π(l)(2)	CASSCF	−1001.454 88	3.658	9.8	104	20.36	40.1
9²Π(g)(2)	CASSCF	−1001.452 34	2.934	8.3	179	20.39	41.7
	MRCI	−1001.504 98	2.895	18.8	226	20.37	22.6
	MRCI+Q	−1001.509 2	2.91	20			20
10⁴Π(2)	CASSCF	−1001.448 01	3.024	9.9	183	20.35	44.4
	MRCI	−1001.504 35	2.937	18.6	219	20.34	23.0
	MRCI+Q	−1001.508 7	2.94	20			21
11²Σ⁺(2)	CASSCF	−1001.470 88	3.509	23.1	117	20.41	30.1
	MRCI	−1001.500 14	3.359	15.5	130	20.44	25.6
	MRCI+Q	−1001.501 7	3.34	15			25
12²Φ(1)	CASSCF	−1001.444 47	2.926	6.9	238	20.30	46.6
	MRCI	−1001.498 56	2.932	15.0	220	20.31	26.6
	MRCI+Q	−1001.502 7	2.94	16			24
13²Π(3)	CASSCF	−1001.445 40	2.931	7.5	202	20.36	46.1
	MRCI	−1001.498 37	2.957	14.9	171	20.40	26.7
	MRCI+Q	−1001.502 3	3.00	16			25
8²Δ(l)(2)	CASSCF	−1001.469 28	3.599	22.6	115	20.39	31.1
	MRCI	−1001.497 49	3.466	14.3	121	20.44	27.3
	MRCI+Q	−1001.499 2	3.44	14			27
14²Δ(3)	CASSCF	−1001.448 06	3.046	12.0	374	20.38	44.4
	MRCI	−1001.495 42	3.291	13.4	284	20.36	28.6
	MRCI+Q	−1001.500 1	3.34	14			26
15⁴Σ⁺(1)	CASSCF	−1001.450 26	4.124	10.5	84	20.26	43.0
	MRCI	−1001.495 40	3.820	13.0	90	20.32	28.6
	MRCI+Q	−1001.498 6	3.75	14			27
16⁴Δ(g)(2)	CASSCF	−1001.436 42	3.355	2.6	110	20.22	51.7
	MRCI	−1001.491 93	3.094	10.9	170	20.29	30.8
	MRCI+Q	−1001.499 4	3.08	14			27
17⁴Π(3)	CASSCF	−1001.436 12	3.665	2.5	111	20.19	51.9
	MRCI	−1001.491 05	3.339	10.3	168	20.33	31.3
	MRCI+Q	−1001.498 0	3.29	13			27
18⁴Σ⁻(g)(2)	CASSCF	−1001.430 61	2.493	21.1	357	20.39	55.3
	MRCI	−1001.490 27	2.533	29.1	325	20.39	31.8
	MRCI+Q	−1001.494 9	2.56	30			29.3
19⁴Σ⁺(2)	CASSCF	−1001.434 49	3.386	2.2	136	20.21	52.9
	MRCI	−1001.487 06	3.332	7.8	204	20.27	33.8
	MRCI+Q	−1001.491 9	3.38	9			31.2
16⁴Δ(l)(2)	CASSCF	−1001.431 45	2.639	−0.5	297	20.30	54.8
	MRCI	−1001.485 03	2.617	6.5	300	20.29	35.1
	MRCI+Q	−1001.488 6	2.62	7			33
18⁴Σ⁻(l)(2)	CASSCF	−1001.420 93	3.726	15.0	84	20.30	61.4
	MRCI	−1001.474 33	3.41	19.1	78	20.34	41.8
20²Σ⁻(2)	CASSCF	−1001.435 63	3.273	8	239	20.23	

[a] Internally contracted MRCI. [b] +Q refers to the multireference Davidson correction, ref 16. [c] The numbers into parenthesis refer to the ordering of states according to energy within the same symmetry manifold.
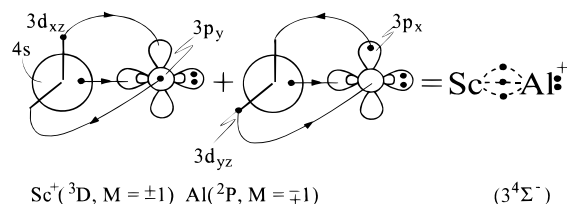
content of about 30 kcal/mol (Table 2) due to the mute role of the symmetry-carrying electron, and with a significant charge transfer of about 0.5 e⁻ from Sc to Al via the σ frame. Bond distances differ by no more than the 0.07 Å with the ²Π having the shortest bond length among the three states. Potential energy curves (PEC) of the states under discussion are shown in Figures 1 and 4.

For the X²Δ and 1²Π states MRCI calculations were also performed without the internal contraction scheme employing the COLUMBUS code.[14] Absolute energies thus obtained are downshifted by 0.89 and 1.3 mhartrees for the X²Δ and 1²Π states, respectively as compared to the internally contracted calculations. However, this energy lowering by about 1 mhartree it is not only caused due to the relaxing of the internal contraction scheme, but also it is due to the fact that our COLUMBUS CASSCF calculations do not possess pure axial symmetry. Although the two sets of calculations, with and without the internal contraction, are practically equivalent, in the latter, the 1²Π ← X²Δ energy separation becomes 0.4 kcal/mol as compared to 0.6 kcal/mol in the former. We observe that going from CASSCF to ic-MRCI to MRCI(no ic), the 1²Π ← X²Δ energy gap diminishes from 8.6 to 0.6 to 0.4 kcal/mol, and finally it is reversed at the icMRCI+Q level (T_e = −0.3 kcal/mol, Table 2), possibly indicating that the ground state is of ²Π symmetry. Calculations done with the augmented basis set on Al (one additional diffuse function for every different angular momentum of the plain Al set) showed imperceptible differences on all calculated properties. Therefore, no other effort was made to extend the basis set size in the rest of the states.

4.2. 3⁴Σ⁻ State. This is the first state that correlates to neutral Al(²P) and Sc⁺(³D), $|3^4\Sigma^-\rangle = |Sc^+, {}^3P; M = \pm 1\rangle \otimes |Al, {}^2P; M = \mp 1\rangle$, as shown in the PEC of Figure 5. There is only one leading equilibrium CASSCF configuration, i.e., $|3^4\Sigma^-\rangle \sim 0.92|1\sigma^2 2\sigma^1 1\pi_x^1 1\pi_y^1\rangle$ with the following atomic distributions, Sc/Al:

$$4s^{0.70}3d_{z^2}^{0.05}3d_{x^2-y^2}^{0.02}3d_{xy}^{0.02}3d_{xz}^{0.74}3d_{yz}^{0.74}4p_x^{0.04}4p_y^{0.04}4p_z^{0.08}/$$
$$3s^{1.72}3p_x^{0.19}3p_y^{0.19}3p_z^{0.39}$$

The obvious vbL icon in conformity with the above description perspicuously suggests the formation of a half σ and two half π bonds:

3d$_{xz}$ 4s 3p$_y$ 3p$_x$ 3d$_{yz}$ = Sc⋮Al⁺

Sc⁺(³D, M = ±1) Al(²P, M = ∓1) (3⁴Σ⁻)

About 0.2 e⁻ is transferred from the metal cation to Al via the σ frame, 0.65 e⁻ is transferred from Al to Sc⁺ through the π frame, and another 0.2 e⁻ is promoted to the 4p orbitals of Sc⁺; overall the Al is losing to Sc⁺ approximately 0.4 e⁻.

The 3⁴Σ⁻ state has a binding energy D_e = 32.6 kcal/mol (MRCI) with respect to Sc⁺(³D) + Al(²P), or 24.1 kcal/mol with respect to the ground state products Sc(²D) + Al⁺(¹S). The bond length of 2.755 Å is shorter than that of the X²Δ state by 0.62 Å, reflecting the bonding character, i.e., three half bonds as compared to the single σ bond of the X²Δ or the 1²Π and 2²Σ⁺ states.

In the isovalent ScB⁺ system[6a] the ground state is of ⁴Σ⁻ symmetry (Figure 2) with, essentially, the same bond character as in the 3⁴Σ⁻ of ScAl⁺: three half bonds but with D_e = 44.9 kcal/mol at R_e = 2.160 Å (MRCI level). The difference between the ScAl⁺ and ScB⁺ bond distances in these states, 2.755−2.160 = 0.60 Å, is equal to the difference between the atomic radii of Al and B, 1.43 and 0.83 Å, respectively.[17] It is also interesting to note that at the ScAl⁺ equilibrium bond distance of 2.76 Å, the X⁴Σ⁻ potential energy curve of ScB⁺ gives a
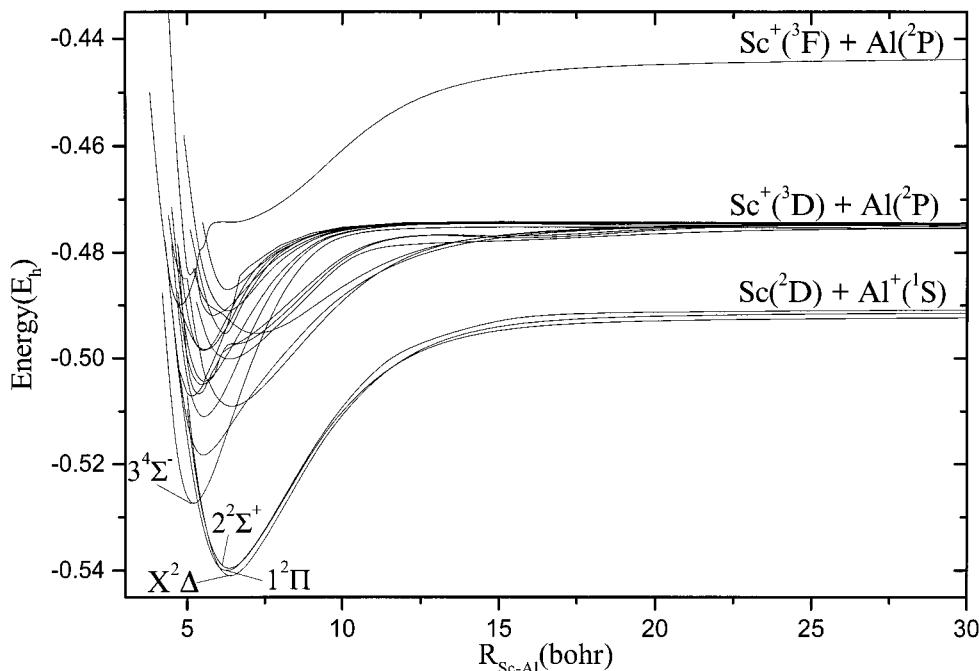
Figure 1. Potential energy curves of all states but the $20^2\Sigma^-$ of the ScAl$^+$ system at the MRCI level of theory.
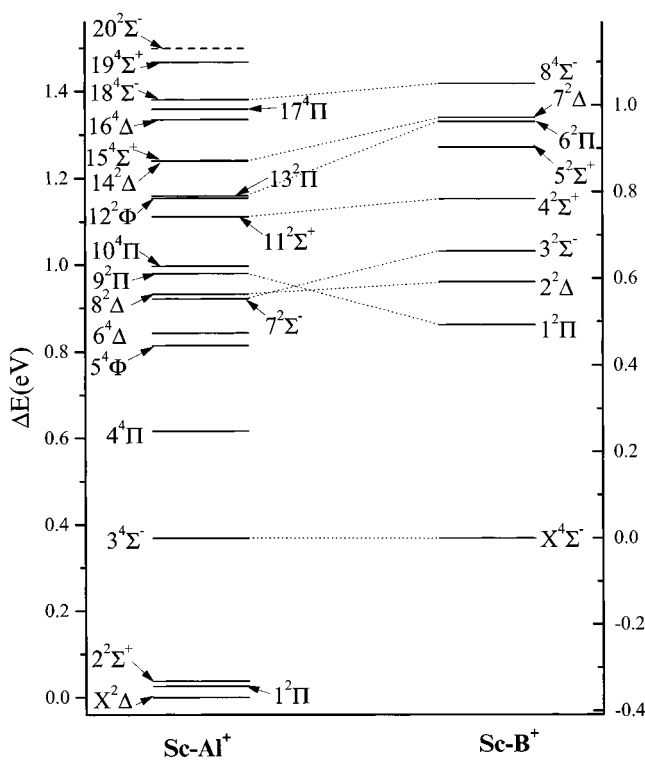

Figure 2. Relative energy levels of the isovalent species ScAl$^+$ and ScB$^+$ at the MRCI level. Thin lines connect similarly bound states of the species.

$$|2^2\Sigma^+\rangle \sim 0.92|1\sigma^2 2\sigma^2 3\sigma^1\rangle$$

binding energy of 30 kcal/mol, very close to 32.6 kcal/mol of the ScAl$^+$ species.

4.3. $7^2\Sigma^-$, $8^2\Delta$, $9^2\Pi$, $11^2\Sigma^+$, $12^2\Phi$, $13^2\Pi$, $14^2\Delta$, and $20^2\Sigma^-$ States. *$7^2\Sigma^-$, $20^2\Sigma^-$.* The $20^2\Sigma^-$ state for purely technical reasons was calculated at the CASSCF level only. However, from the MRCI potential energy curve of the $7^2\Sigma^-$ state (Figure 3), it is clear that there is an avoided crossing between these two states (vide infra). The $7^2\Sigma^-$ was state averaged at the

CASSCF level with the X$^2\Delta$ and $8^2\Delta$ states, and around the equilibrium it was extracted as second root of the MRCI matrix. Asymptotically the $7^2\Sigma^-$ wave function is described by the product wave function $|7^2\Sigma^-\rangle = |\text{Sc}^+, {}^3\text{D}; M = \pm1\rangle \otimes |\text{Al}, {}^2\text{P}; M = \mp1\rangle$; upon the approach of the two atoms and around 6.3 bohr, the above asymptotic character changes due to an avoided crossing with the incoming $20^2\Sigma^-$ state which correlates to $|\text{Sc}^+, {}^1\text{D}; M = \pm1\rangle \otimes |\text{Al}, {}^2\text{P}; M = \mp1\rangle$ (see inset of Figure 3). Thus, at the equilibrium distance the in situ Sc$^+$ atom carries the memory of the ^{1}D ($M = \pm1$) atomic state.

At the equilibrium, and at the CASSCF level, the leading configuration functions are

$$|7^2\Sigma^-\rangle \sim 0.74|1\sigma^2 2\bar{\sigma}^1 1\pi_x^1 1\pi_y^1\rangle + 0.37(|1\sigma^2 2\sigma^1 1\bar{\pi}_x^1 1\pi_y^1\rangle + |1\sigma^2 2\sigma^1 1\pi_x^1 1\bar{\pi}_y^1\rangle)$$

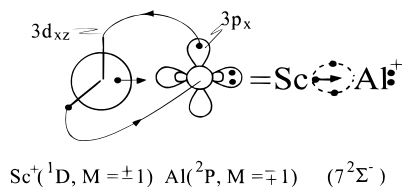and with the CAS atomic population distributions (Sc/Al),

$$4s^{0.78} 3d_{z^2}^{0.07} 3d_{x^2-y^2}^{0.02} 3d_{xy}^{0.02} 3d_{xz}^{0.67} 3d_{yz}^{0.67} 4p_x^{0.04} 4p_y^{0.04} 4p_z^{0.11}/$$
$$3s^{1.56} 3p_x^{029} 3p_y^{0.29} 3p_z^{0.37}$$

At infinity, the atomic states are represented by the following combinations

$$|\text{Sc}^+, {}^1\text{D}; M=1\rangle = 1/\sqrt{2}[|4s^1(3\bar{d}_{xz} + i3\bar{d}_{yz})^1\rangle - |4\bar{s}^1(3d_{xz} + i3d_{yz})^1\rangle]$$

$$|\text{Al}, {}^2\text{P}; M=-1\rangle = 1/\sqrt{2}[|3s^2 p_x^1\rangle - i|3s^2 p_y^1\rangle]$$

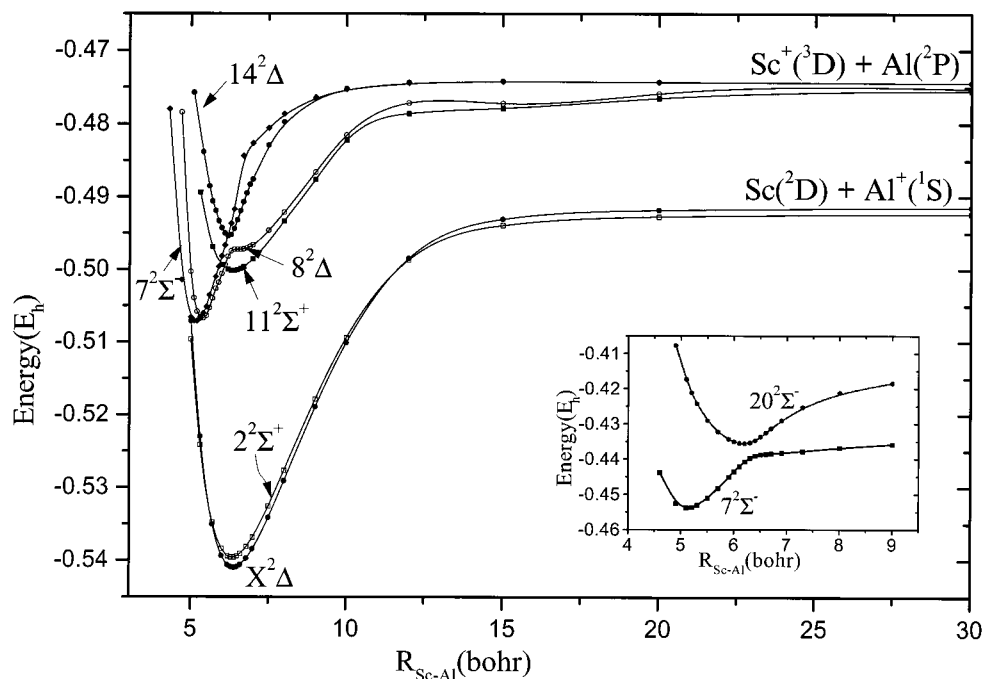showing that the bonding can be represented by the vbL icon:

Sc$^+$(^{1}D, M $=\pm$1)$\cdot$ Al(^{2}P, M $=\mp$1)   ($7^2\Sigma^-$)

Figure 3. MRCI potential energy curves of Δ, Σ^+, and Σ^- doublets. Inset: CASSCF PECs of $7^2\Sigma^-$ and $20^2\Sigma^-$ states (see text).
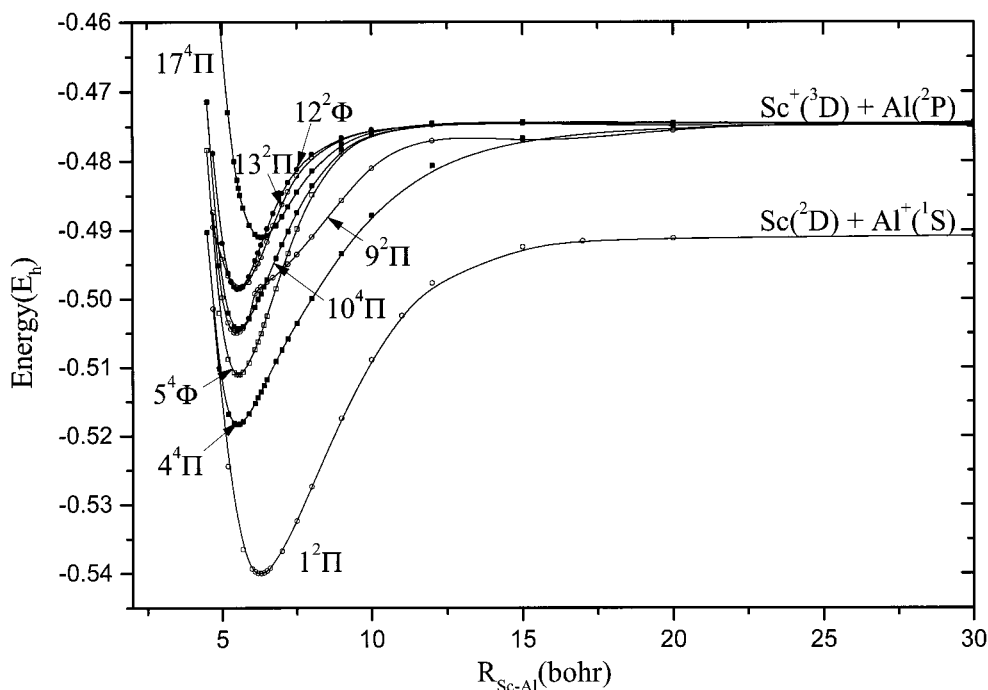

Figure 4. Potential energy curves of doublets and quartets of Π and Φ symmetries at the MRCI level.

The above diagram indicates the formation of two half π bonds and one putative half σ bond as is evinced from the CAS equilibrium Mulliken populations, and the asympotic population distributions of Sc$^+$ and Al. 0.4 e$^-$ are transferred from Al to the Sc$^+$ atom via the π frame, while no charge transfer is observed from the Sc$^+$($4s3d_{z^2}4p_z$)$^{0.78+0.07+0.11}$ hybrid toward the Al (sp$_z$)$^{1.56+0.37}$ hybrid.

The bond distance, one of the smallest of all states studied, is 2.702 Å with a D_e = 20.3 kcal/mol with respect to the adiabatic products, Sc$^+$(^{3}D) + Al(^{2}P). However, with respect to the *diabatic* fragments, Sc$^+$(^{1}D) + Al(^{2}P), the *intrinsic bond strength* is 20.3 + Sc$^+$(^{1}D←^{3}D) = 26.3 kcal/mol (Tables 1 and 2). *Mutatis-mutandis* the same situation holds in the first $^2\Sigma^-$ state of the ScB$^+$ molecule with a D_e = 27.4 kcal/mol at R_e =

2.167 Å, and an analogous avoided crossing with the next $^2\Sigma^-$ state of ScB$^+$.[6a]

As already mentioned, the *$20^2\Sigma^-$ state* has been obtained only at the CASSCF level of theory, showing the avoided crossing with the $7^2\Sigma^-$ previously discussed (see Figure 3). The leading CAS equilibrium configurations and corresponding Mulliken distributions are

$$20^2\Sigma^- \sim 0.43(|1\sigma^2 2\sigma^1 1\bar{\pi}_x^1 1\pi_y^1\rangle + |1\sigma^2 2\sigma^1 1\pi_x^1 1\bar{\pi}_y^1\rangle) -$$
$$0.42(|1\sigma^2 2\sigma^1 2\bar{\pi}_x^1 2\pi_y^1\rangle + |1\sigma^2 2\sigma^1 2\pi_x^1 2\bar{\pi}_y^1\rangle)$$

$$4s^{0.98}3d_{z^2}^{0.05}3d_{xz}^{0.53}3d_{yz}^{0.53}4p_x^{0.02}4p_y^{0.02}4p_z^{0.09}/3s^{1.65}3p_z^{045}3p_y^{0.45}3p_z^{0.17}$$
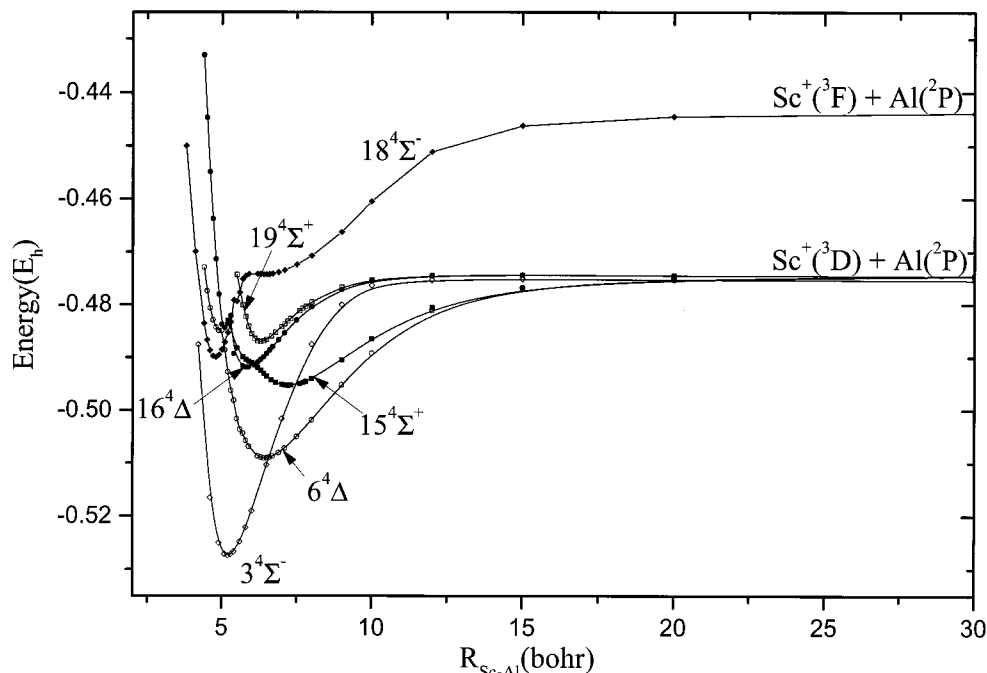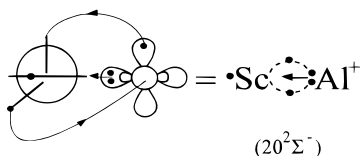
leading to the following bonding vbL picture

6866 *J. Phys. Chem. A, Vol. 104, No. 29, 2000*

Tzeli and Mavridis

Figure 5. Potential energy curves of Δ, Σ^+, and Σ^- quartets of ScAl$^+$ at the MRCI level of theory.

$$(20\,^2\Sigma^-)$$

The bonding is composed of two half π bonds and a putative σ bond; about 0.1 and 0.15 e$^-$ move from Al to Sc$^+$ through the π and σ frames, respectively. At the CASSCF equilibrium bond length of 3.273 Å a D_e = 8 kcal/mol with respect to Sc$^+$-(^{3}D) + Al(^{2}P) is recorded, Table 2.

$8^2\Delta$, $14^2\Delta$. Both states trace their origin to |Sc$^+$, ^{3}D; $M = \pm 2, \pm 1\rangle \otimes$ |Al, ^{2}P; $M = 0, \pm 1\rangle$ atomic states, Figure 3. However, the interaction between the two atoms is more compounded than it appears to be in the PECs, so to glean some insight of the bonding mechanism we have to follow the evolution of the potential energy curves from infinity to the equilibrium geometry. At this point it should be mentioned that both states have been computed as a state average of X$^2\Delta$, $8^2\Delta$, $14^2\Delta$, and $7^2\Sigma^-$ states employing a $w(1,1,1,1)$ weighing vector, but for the local minimum around 6.2 bohr a state average of X$^2\Delta$, $8^2\Delta$, $2^2\Sigma^+$, and $11^2\Sigma^+$ states was used.

Now the $8^2\Delta$ state and up to about an interatomic distance of 12 bohr exhibits its asymptotic character, i.e., Sc$^+$(^{3}D; $M = \pm 2$) + Al(^{2}P; $M = 0$). Moving further to the left, it experiences an avoided crossing with an incoming $^2\Delta$ state (Figure 3), correlating to Sc$^+$(^{1}D; $M = \pm 2$) + Al(^{2}P; $M = 0$). This character is carried to the PEC local minimum ($R = 3.466$ Å), where it suffers a second avoided crossing with the $14^2\Delta$ state; therefore, at equilibrium its character changes again to Sc$^+$(^{3}D; $M = \pm 1$) + Al(^{2}P; $M = \pm 1$).
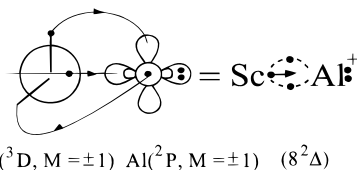
At the global minimum (equilibrium) the CASSCF leading configurations and atomic distributions are

$$|8^2\Delta\rangle \sim 0.62(|1\sigma^2 2\sigma^1 1\bar{\pi}_x^1 1\pi_y^1\rangle - |1\sigma^2 2\sigma^1 1\pi_x^1 1\bar{\pi}_y^1\rangle)$$

$$4s^{0.78}3d_{z^2}^{0.06}3d_{x^2-y^2}^{0.02}3d_{xy}^{0.02}3d_{xz}^{0.67}3d_{yz}^{0.67}4p_x^{0.03}4p_y^{0.03}4p_z^{0.10}/$$
$$3s^{1.61}3p_x^{028}3p_y^{0.28}3p_z^{0.40}$$

The bonding can be represented rather faithfully by the vbL icon

Sc$^+$(^{3}D, $M = \pm 1$) Al(^{2}P, $M = \pm 1$) $(8\,^2\Delta)$

suggesting two half π bonds and perhaps a putative half σ bond. About 0.4 e$^-$ is diffused via the π skeleton from Al to Sc$^+$, while along the σ frame both atoms retain their electron counts: about 1 e$^-$ resides on a $(4s4p_z)^{0.78+0.10}$ hybrid and 2 e$^-$ on a $(3s3p_z)^{1.61+0.40}$ Al hybrid.

At the MRCI level of theory we predict a binding energy D_e = 20.1 kcal/mol at R_e = 2.844 Å relative to Sc$^+$(^{3}D) + Al(^{2}P), Table 2. The bonding is very similar to the corresponding $1^2\Delta$ state of the isovalent ScB$^+$ species,[6a] where also due to an avoided crossing the global minimum carries the memory of a Sc$^+$(^{3}D; $M = \pm 1$) + B(^{2}P; $M = \pm 1$) fragment. Due to the smaller atomic radius of B, a smaller equilibrium distance R_e-(ScB$^+$, $1^2\Delta$) = 2.233 Å is recorded, with a synchronous development of a half σ bond and D_e = 29.1 kcal/mol.

The $14^2\Delta$ *state* correlating to Sc$^+$(^{3}D; $M = \pm 1$) + Al(^{2}P; $M = \pm 1$) suffers an intense avoided crossing at 6.3 bohr with the previously discussed $8^2\Delta$ state, Figure 3. As a result, the equilibrium character of the $14^2\Delta$ state is mainly represented by Sc$^+$(^{3}D; $M = \pm 2$) + Al(^{2}P; $M = 0$). The leading CASSCF equilibrium CFs and population distributions are

$$|14^2\Delta\rangle \sim 0.81|1\sigma^2 2\sigma^1 3\sigma^1 1\delta_-^1\rangle - 0.33|1\sigma^2 2\sigma^1 1\pi_x^1 1\bar{\pi}_y^1\rangle +$$
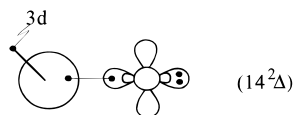$$0.19|1\sigma^2 2\sigma^1 1\bar{\pi}_x^1 1\pi_y^1\rangle$$

$$4s^{0.82}3d_{z^2}^{0.17}3d_{xy}^{0.76}3d_{xz}^{0.17}3d_{yz}^{0.17}4p_x^{0.01}4p_y^{0.01}4p_z^{0.25}/$$
$$3s^{1.75}3p_x^{0.10}3p_y^{0.10}3p_z^{0.58}$$

Due to the avoided crossing, the contamination at equilibrium from Sc$^+$(^{3}D; $M = \pm 1$) is reflected in the above population

Electronic Structure of ScAl$^+$

J. Phys. Chem. A, Vol. 104, No. 29, 2000 **6867**

distributions. The electron count of $3d_{xy}$ ($M = \pm 2$) is 0.76 instead of 1.0, with 0.34 e$^-$ residing on $3d_{xz} + 3d_{yz}$ orbitals, revealing the entanglement of the Sc$^+$(^{3}D; $M = \pm 1$) state. Again, because of the avoided crossing no clear vbL picture can be drawn; the bonding can be represented by a $\sim(0.81)^2 = 0.65$ component of the icon

$$(14\,^2\Delta)$$

plus a ~ 0.35 component of the previously reported icon of the $8\,^2\Delta$ state.

For the $14\,^2\Delta$ state the D_e and R_e MRCI values are 13.4 kcal/mol and 3.291 Å, respectively, with a total electron migration of 0.40 e$^-$ from Al to Sc$^+$.
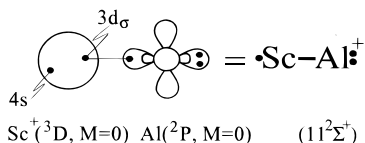
$11\,^2\Sigma^+$. It was computed as a state average of three more states, namely, X$^2\Delta$, $2\,^2\Sigma^+$, and $8\,^2\Delta$, and at infinity can be described by the product wave function $|$Sc$^+$, ^{3}D; $M = 0\rangle \otimes |$Al, ^{2}P; $M = 0\rangle$, Figure 3. The main CASSCF equilibrium CFs are

$$|11\,^2\Sigma^+\rangle \sim 0.78|1\sigma^2 2\sigma^1 3\sigma^2\rangle + 0.35|1\sigma^2 2\sigma^1 4\sigma^2\rangle$$

with corresponding Mulliken populations

$$4s^{0.99}3d_{z^2}^{1.13}3d_{x^2-y^2}^{0.02}3d_{xy}^{0.02}4p_z^{0.25}/3s^{1.81}3p_x^{0.05}3p_y^{0.05}3p_z^{0.65}$$

and a total of 0.40 e$^-$ transferred from Al to Sc$^+$ via the σ frame. The two atoms are held together, practically, by a σ bond ("$3\sigma^2$") formed between the $3d_{z^2}$ and $3p_z$ atomic orbitals of Sc$^+$ and Al, with the single electron ("$2\sigma^1$") hosted on a rather undisturbed 4s Sc$^+$ atomic function. The above observations can be captured in the following vbL picture:

$$\text{Sc}^+(^3\text{D, M=0}) \quad \text{Al}(^2\text{P, M=0}) \qquad (11\,^2\Sigma^+)$$

The MRCI D_e and R_e values (Table 2), are 15.5 kcal/mol and 3.359 Å, respectively.

Although in a similar state ($1\,^2\Sigma^+$) of the ScB$^+$ the potential energy curve presents two minima due to an avoided crossing,[6a] the global minimum has similar bonding features with the present $11\,^2\Sigma^+$ ScAl$^+$ state, presenting a rather weak σ bond ($D_e = 24.6$ kcal/mol) at a distance of 2.816 Å.

$9\,^2\Pi$, $13\,^2\Pi$, $12\,^2\Phi$. These states trace their lineage to the asymptotic products $|$Sc$^+$, ^{3}D; $M = \pm 1, \pm 2, \pm 2\rangle \otimes |$Al, ^{2}P; $M = 0, \mp 1, \pm 1\rangle$. The $9\,^2\Pi$ state was state averaged with the $1\,^2\Pi$ state while the $13\,^2\Pi$ and $12\,^2\Phi$ states have been obtained from a state average of four states, namely, $1\,^2\Pi$, $9\,^2\Pi$, $13\,^2\Pi$, and $12\,^2\Phi$ with a $w(1,1,1,1)$ statistical vector. Figure 4 shows the corresponding potential energy curves.

The *$9\,^2\Pi$ state*, and within the range of 12−10 bohr, interacts strongly with a higher $^2\Pi$ state correlating to Sc$^+$(^{1}D; $M = \pm 1$) + Al(^{2}P; $M = 0$). Subsequently, and as we move toward the equilibrium, at about 6.1 bohr the PEC changes abruptly its slope, possibly due to an avoided crossing with another $^2\Pi$ state (but clearly not with the $13\,^2\Pi$), the origin of which we were unable to locate unambiguously.

The main CASSCF configurations with the corresponding Mulliken populations are (B$_1$ component)

$$|9\,^2\Pi\rangle \sim 0.61|1\sigma^2 2\sigma^1 3\sigma^1 1\bar{\pi}_x^1\rangle - 0.43|1\sigma^2 2\sigma^1 3\bar{\sigma}^1 1\pi_x^1\rangle +$$
$$0.23(|1\sigma^2 2\sigma^1 1\pi_y^1 1\delta_-^1\rangle - |1\sigma^2 2\sigma^1 1\pi_x^1 \bar{\delta}_+^1\rangle)$$

$$4s^{0.85}3d_{z^2}^{0.60}3d_{x^2-y^2}^{0.12}3d_{xy}^{0.11}3d_{xz}^{0.25}3d_{yz}^{0.25}4p_x^{0.03}4p_y^{0.03}4p_z^{0.13}/$$
$$3s^{1.66}3p_x^{0.24}3p_y^{0.24}3p_z^{0.45}$$

Taking also into account the detailed form of the CAS orbitals $1\sigma \sim 3s_{\text{Al}}$, $2\sigma \sim (0.70)4s_{\text{Sc}} - (0.46)3s_{\text{Al}} - (0.70)3p_{z,\text{Al}}$, $3\sigma \sim (-0.73)3d_{z^2,\text{Sc}} + (0.56)3p_{z,\text{Al}}$, and $1\pi_x \sim (0.68)3d_{xz,\text{Sc}} + (0.72)3p_{x,\text{Al}}$, we can draw, certainly with some reservations, the following vbL equilibrium picture

$$(9\,^2\Pi)$$

suggesting a half σ and a half π bond. The D_e and R_e values are 18.8 kcal/mol and 2.895 Å, respectively with an overall transfer of 0.4 e$^-$ from Al to Sc$^+$.

States *$13\,^2\Pi$ and $12\,^2\Phi$* are degenerate within the accuracy of our calculations and have, practically, very similar potential energy curves, Figure 4. Both states present avoided crossings at about 7 bohr as evidenced from the complete dominance of the asymptotic Sc$^+$(^{1}D; $M = \pm 2$) $\otimes$ Al(^{2}P; $M = \mp 1, \pm 1$) atomic states for the Π and Φ vectors, respectively; therefore the bonding at equilibrium carries the character of the Sc$^+$(^{1}D) instead of the Sc$^+$(^{3}D) asymptote.
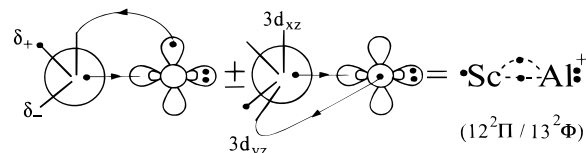
The leading CAS equilibrium configurations (B$_1$ components) are

$$|13\,^2\Pi\rangle \sim 0.43(|1\sigma^2 2\sigma^1 1\pi_y^1 1\bar{\delta}_-^1\rangle - |1\sigma^2 2\sigma^1 1\bar{\delta}_+^1 1\pi_x^1\rangle) -$$
$$0.30(|1\sigma^2 2\bar{\sigma}^1 1\pi_y^1 1\delta_-^1\rangle - |1\sigma^2 2\bar{\sigma}^1 1\delta_+^1 1\pi_x^1\rangle)$$

$$|12\,^2\Phi\rangle \sim 0.51(|1\sigma^2 2\sigma^1 1\pi_y^1 1\bar{\delta}_-^1\rangle + |1\sigma^2 2\sigma^1 1\bar{\delta}_+^1 1\pi_x^1\rangle) -$$
$$0.38(|1\sigma^2 2\bar{\sigma}^1 1\pi_y^1 1\delta_-^1\rangle + |1\sigma^2 2\bar{\sigma}^1 1\delta_+^1 1\pi_x^1\rangle)$$

with corresponding CAS atomic populations as follows:

$$4s^{0.74}3d_{z^2}^{0.30}3d_{x2-y2}^{0.33}3d_{xy}^{0.33}3d_{xz}^{0.23}3d_{yz}^{0.23}4p_x^{0.01}4p_y^{0.01}4p_z^{0.11}/$$
$$3s^{1.64}3p_x^{0.28}3p_y^{0.28}3p_z^{0.42}$$

$$4s^{0.70}3d_{z^2}^{0.10}3d_{x^2-y^2}^{0.50}3d_{xy}^{0.50}3d_{xz}^{0.16}3d_{yz}^{0.16}4p_x^{0.04}4p_y^{0.04}4p_z^{0.10}/$$
$$3s^{1.62}3p_x^{0.32}3p_y^{0.32}3p_z^{0.41}$$

The Sc population differences between the two states are due to the contamination of the $13\,^2\Pi$ state with the previously described $9\,^2\Pi$ state. The bonding, for both states, can be represented by the same vbL icons (B$_1$ symmetry)

$$(12\,^2\Pi\,/\,13\,^2\Phi)$$

with the ''−'' and ''+'' corresponding to the Π and Φ symmetries, respectively. In both states the two atoms are glued together by two half bonds, a σ and a π. In the Φ state 0.36 e$^-$ migrates from Al to Sc through the σ frame, resulting in a total

transfer from Al to Sc$^+$ of 0.30 e$^-$; practically the same holds true for the Π state. As shown in Table 2, the binding energies and bond distances are D_e = 14.9 and 15 kcal/mol, R_e = 2.957 and 2.932 Å, for the $13^2\Pi$ and $12^2\Phi$ states, respectively.
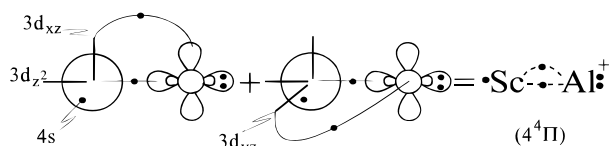
4.4. $4^4\Pi$, $5^4\Phi$, $6^4\Delta$, $10^4\Pi$, $15^4\Sigma^+$, $16^4\Delta$, $17^4\Pi$, $18^4\Sigma^-$ and $19^4\Sigma^+$ States. *$4^4\Pi$, $5^4\Phi$, $10^4\Pi$, $17^4\Pi$.* All four states have been state averaged with a $w(1,1,1,1)$ weighting vector, and all trace their ancestry to Sc$^+$(^{2}D) + Al(^{2}P) atomic fragments, Figure 4.

At infinity the *$4^4\Pi$ state* (the lowest of the Π's) is described by the product wave function |Sc$^+$, ^{3}D; M_L = ±1⟩ ⊗ |Al, ^{2}P; M_L = 0⟩. At the equilibrium the CASSCF leading configuration and Mulliken populations are

$$|4^4\Pi\rangle \sim 0.78|1/\sqrt{2}[1\sigma^2 2\sigma^1 3\sigma^1(1\pi_x^1 + 1\pi_y^1)]\rangle$$

$$4s^{0.90}3d_{z^2}^{0.61}3d_{x^2-y^2}^{0.10}3d_{xy}^{0.10}3d_{xz}^{0.28}3d_{yz}^{0.28}4p_z^{0.13}/3s^{1.72}3p_x^{0.22}3p_y^{0.22}3p_z^{0.39}$$

Taking also into account the asymptotic populations ($4s^1d_{xz}^{0.5}d_{xz}^{0.5}/3s^{1.92}3p_z^13p_x^{0.04}3p_y^{0.04}$), the bonding character can be pictured as a superposition of two vbL icons

$$(4^4\Pi)$$

indicating that the bonding is composed of two half bonds, a σ and a π, with the 4s($\sim$2σ) electron being essentially indifferent to the bonding process. Via the π skeleton 0.36 e$^-$ is transferred from Sc$^+$ to Al while 0.81 e$^-$ moves back through the σ frame, amounting to a total migration of about 0.5 e$^-$ from Al to Sc$^+$. A binding energy of 27.6 kcal/mol is predicted at R_e = 2.917 Å at the MRCI level, Table 2.

The *$5^4\Phi$ and $10^4\Pi$ states* correlate to |Sc$^+$, ^{3}D; M_L = ±2⟩ ⊗ |Al, ^{2}P; M_L = ±1, ∓1⟩ product states, with their PECs at the MRCI level shown in Figure 4. The dominant CASSCF equilibrium configurations (B$_1$ symmetry) are

$$|5^4\Phi\rangle \sim 0.67(|1\sigma^2 2\sigma^1 1\delta_+^1 1\pi_x^1\rangle + |1\sigma^2 2\sigma^1 1\pi_y^1 1\delta_-^1\rangle)$$

$$|10^4\Pi\rangle \sim 0.60(|1\sigma^2 2\sigma^1 1\delta_+^1 1\pi_x^1\rangle - |1\sigma^2 2\sigma^1 1\pi_y^1 1\delta_-^1\rangle) + 0.38|1\sigma^2 2\sigma^1 3\sigma^1 1\pi_x^1\rangle$$

with the 0.38 component of the $10^4\Pi$ state carrying the character of the previously described $4^4\Pi$ state (vide supra). Of course, the B$_2$ components are completely symmetrical; i.e., the π_x orbitals are replaced by π_y and vice versa.

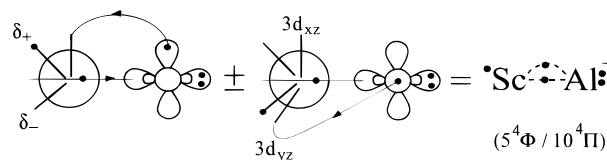Corresponding atomic Mulliken CAS distributions are as follows:

$5^4\Phi$:
$$4s^{0.76}3d_{z^2}^{0.08}3d_{x^2-y^2}^{0.50}3d_{xy}^{0.50}3d_{xz}^{0.18}3d_{yz}^{0.18}4p_x^{0.01}4p_y^{0.01}4p_z^{0.10}/$$
$$3s^{1.67}3p_x^{0.29}3p_y^{0.29}3p_z^{0.34}$$

$10^4\Pi$:
$$4s^{0.89}3d_{z^2}^{0.20}3d_{x^2-y^2}^{0.40}3d_{xy}^{0.40}3d_{xz}^{0.14}3d_{yz}^{0.14}4p_x^{0.01}4p_y^{0.01}4p_z^{0.10}/$$
$$3s^{1.68}3p_x^{0.34}3p_y^{0.34}3p_z^{0.27}$$

The bonding can be clearly represented by the following vbL picture (B$_1$symmetry)
implying two half bonds of σ and π character, and a nonparticipating in the bonding process (observer) electron of δ_+ (or

$$(5^4\Phi / 10^4\Pi)$$

δ_-) symmetry. The "+" sign corresponds to the Φ symmetry and the "−" to the Π symmetry. A total charge of 0.38 and 0.35 e$^-$ is transferred from Al to Sc$^+$ in the Φ and Π symmetries, practically via the π frame only. As expected, bond distances and dissociation energies of these two states are very similar: R_e = 2.930 and 2.937 Å and D_e = 22.8 and 18.6 kcal/mol for the Φ and Π states, respectively (Table 2).
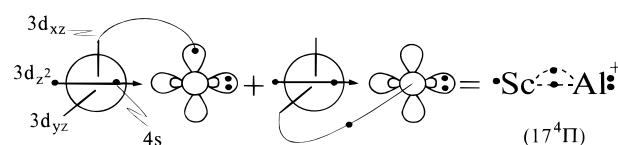
The *$17^4\Pi$ state* at infinity is represented by the wave function |Sc$^+$, ^{3}D; M_L = 0⟩ ⊗ |Al, ^{2}P; M_L = ±1⟩, with switched M values as compared to the $4^4\Pi$ state (vide supra); its PEC is shown in Figure 4. The equilibrium CASSCF wave function has two main components:

$$|17^4\Pi\rangle \sim 0.70[1/\sqrt{2}(|1\sigma^2 2\sigma^1 4\sigma^1 1\pi_x^1\rangle + |1\sigma^2 2\sigma^1 4\sigma^1 1\pi_y^1\rangle)] + 0.47[1/\sqrt{2}(|1\sigma^2 2\sigma^1 3\sigma^1 1\pi_x^1\rangle + |1\sigma^2 2\sigma^1 3\sigma^1 1\pi_y^1\rangle)]$$

the second of which owes its presence to the mixing with the $4^4\Pi$ state. The Mulliken CAS populations are (Sc/Al)

$$4s^{1.01}3d_{x^2}^{0.83}3d_{xz}^{0.11}3d_{yz}^{0.11}4p_x^{0.0}4p_y^{0.0}4p_z^{0.08}/3s^{1.82}3p_x^{0.39}3p_y^{0.39}3p_z^{0.20}$$

and, disregarding the "0.47" component, suggest the following binding scheme:

$$(17^4\Pi)$$

The two atoms are, practically, connected with a half π bond while a net transfer of 0.2 e$^-$ from Al to Sc$^+$ takes place through the π system. This obviously weak bonding interaction is reflected to the small dissociation energy, D_e = 10.3 kcal/mol at R_e = 3.339 Å (MRCI level, Table 2). Notice also that this is the first unbound excited state (by 0.2 kcal/mol) with respect to Sc(^{2}D) + Al$^+$(^{1}S).

$6^4\Delta$, $16^4\Delta$, $18^4\Sigma^-$, $15^4\Sigma^+$, $19^4\Sigma^+$. With the exception of the $18^4\Sigma^-$, the rest of the states correlate to the ground state atoms, Sc$^+$(^{3}D) + Al(^{2}P). The asymptotic wave functions are given by the product atomic functions |Sc$^+$, ^{3}D; M = ±2, ±1, 0, ±1⟩ ⊗ |Al, ^{2}P; M = 0, ±1, 0, ∓1⟩ for the $6^4\Delta$, $16^4\Delta$, $15^4\Sigma^+$, and $19^4\Sigma^+$ states, respectively.

The *$6^4\Delta$ state* was calculated as a state average with the $3^4\Sigma^-$ described earlier. The CASSCF wave function of the $6^4\Delta$ is practically the sum of the two CFs of symmetries A$_1$ and A$_2$
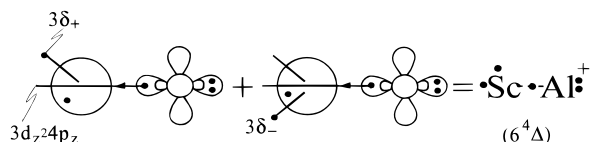
$$0.97\{1/\sqrt{2}(|1\sigma^2 2\sigma^1 3\sigma^1 1\delta_+^1\rangle + |1\sigma^2 2\sigma^1 3\sigma^1 1\delta_-^1\rangle)\}$$

The Mulliken equilibrium populations differ slightly from their asymptotic counterparts due to a transfer of about 0.4 e$^-$ from Al to Sc$^+$ along the σ frame:

$$4s^{0.99}3d_{z^2}^{0.15}3d_{x^2-y^2}^{0.50}3d_{xy}^{0.50}4p_z^{0.27}/3s^{1.83}3p_x^{0.03}3p_y^{0.03}3p_z^{0.67}$$

The relatively strong binding, D_e = 21.6 kcal/mol at R_e = 3.387 Å, is caused by a half σ bond originating from the interaction of the 3p$_z$ (Al) and 3d$_{z^2}$4p$_z$ hybrid orbital on Sc$^+$,

Electronic Structure of ScAl⁺

J. Phys. Chem. A, Vol. 104, No. 29, 2000 **6869**

with no participation of the 4s e⁻. The bonding mechanism is captured by the following vbL picture:

$$(6\,^4\Delta)$$

The developing local minimum in the repulsive part and around 4.9 bohr of this state's PEC shown in Figure 5 owes its existence to an avoided crossing with $16\,^4\Delta$ state correlating, in this region, to Sc⁺(^{3}F; $M = \mp3$ or ±1) + Al(^{2}P; $M = \pm1$).

Finally, it should be mentioned that the $6\,^4\Delta$ state was also explored employing an "augmented" (by one a₁, 4p$_z$ on Sc⁺ symmetry function) reference space resulting in a 11-function CASSCF. The result was an insignificant increase by 0.11 kcal/mol in D_e, so this point was not pursued any further.

Figure 5 shows the MRCI potential energy curve of the $16\,^4\Delta$ *state* produced by state averaging the $3\,^4\Sigma^-$, $6\,^4\Delta$, $16\,^4\Delta$, and $18\,^4\Sigma^-$ states with a $w(1,1,1,1)$ weighing vector. At about 5.3 bohr an avoided crossing occurs with an incoming (not computed) $^4\Delta$ state (see previous $6\,^4\Delta$ description), correlating to Sc⁺(^{3}F; $M = \mp3$ or ±1) + Al(^{2}P; $M = \pm1$), while a second avoided crossing occurs at 4.9 bohr with the previously described $6\,^4\Delta$ state. The local minimum is at $R_e = 2.617$ Å, Table 2. The dominant equilibrium CASSCF configurations for the local (l) and global (g) minima are

$$|6\,^4\Delta\rangle_g = 0.69/\sqrt{2}[(|1\sigma^2 2^1 1\pi_x^1 2\pi_x^1\rangle - |1\sigma^2 2\sigma^1 1\pi_y^1 2\pi_y^1\rangle) +$$
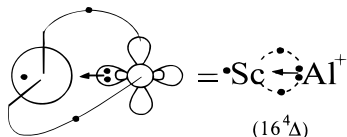$$(|1\sigma^2 2\sigma^1 1\pi_x^1 2\pi_x^1\rangle - |1\sigma^2 2\sigma^1 2\pi_x^1 1\pi_y^1\rangle)]$$

$$|6\,^4\Delta\rangle_l = 0.97/\sqrt{2}(|1\sigma^2 1\pi_x^1 1\pi_y^1 1\delta_-^1\rangle + |1\sigma^2 1\delta_+^1 1\pi_x^1 1\pi_y^1\rangle)$$

Notice the presence of the A₁ and A₂ symmetries on the above wave functions resulting in pure axial Δ symmetry. The corresponding Mulliken distributions for the local and global minima are

g: $4s^{1.01} 3d_{z^2}^{0.06} 3d_{xz}^{0.51} 3d_{yz}^{0.51} 4p_x^{0.02} 4p_y^{0.02} 4p_z^{0.08}/$
$$3s^{1.71} 3p_x^{0.48} 3p_y^{0.48} 3p_z^{0.09}$$

l: $4s^{0.14} 3d_{z^2}^{0.08} 3d_{x^2-y^2}^{0.50} 3d_{xy}^{0.50} 3d_{xz}^{0.43} 3d_{yz}^{0.43} 4p_x^{0.07} 4p_y^{0.07} 4p_z^{0.08}/$
$$3s^{1.62} 3p_x^{0.48} 3p_y^{0.48} 3p_z^{0.06}$$

At equilibrium the bonding in the "g" minimum can be represented by the following picture

$$(16\,^4\Delta)$$

implying two half π bonds and a putative σ bond, with practically no transfer of e⁻ through the π frame but with 0.15 e⁻ moving from Al to Sc⁺ via the σ frame. At the MRCI level a D_e of 10.9 kcal/mol and an R_e of 3.094 Å are obtained.

The "l" minimum has a well depth of 2.84 mhartree or 623 cm⁻¹ with an $\omega_e = 300$ cm⁻¹ (Table 2), possibly sustaining two vibrational levels before "leaking" to the "g" minimum. At the equilibrium distance of 2.62 Å, the D_e with respect to Sc⁺(^{3}D; $M = \pm1$) + Al(^{2}P; $M = \pm1$) is 6.5 kcal/mol, but its

intrinsic bond strength, that is, with respect to the diabatic fragments Sc⁺(^{3}F; $M = \mp3$ or ±1) + Al(^{2}P; $M = \pm1$), is 6.5 + $\Delta E(^3$F←^{3}D) = 6.5 + 16.2 = 22.7 kcal/mol.

Figure 5 shows the $18\,^4\Sigma^-$ *state* PEC correlating to Sc⁺(^{3}F; $M = 0$) + Al(^{2}P; $M = 0$), and suffering an avoided crossing around 5.9 bohr with an incoming (not computed) $^4\Sigma^-$ state correlating to Sc⁺(^{3}F; $M = \pm1$) + Al(^{2}P; $M = \mp1$). Due to the avoided crossing, there is a local minimum at $R_e = 3.41$ Å barely sustaining a single vibration and a global minimum at $R_e = 2.533$ Å, the shortest bond length of all states studied, with $D_e = 29.1$ kcal/mol with respect to the adiabatic fragments.

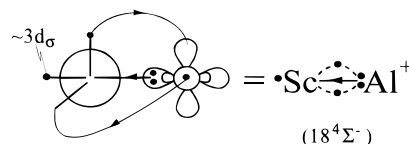At equilibrium the leading CASSSCF configurations are

$$|18\,^4\Sigma^-\rangle \sim 0.89|1\sigma^2 3\sigma^1 1\pi_x^1 1\pi_y^1\rangle + 0.23|1\sigma^2 2\sigma^1 1\pi_x^1 1\pi_y^1\rangle$$

with the following atomic distributions:

$4s^{0.38} 3d_{z^2}^{0.72} 3d_{x^2-y^2}^{0.01} 3d_{xy}^{0.01} 3d_{xz}^{0.48} 3d_{yz}^{0.48} 4p_x^{0.08} 4p_y^{0.08} 4p_z^{0.10}/$
$$3s^{1.59} 3p_x^{0.40} 3p_y^{0.40} 3p_z^{0.14}$$

The "0.23" component corresponds to the $3\,^4\Sigma^-$ state previously discussed.
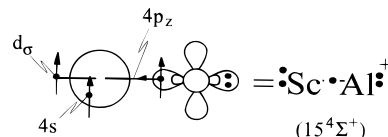
Taking into account the character change of the Sc⁺ and Al species due to the avoided crossing from $M = (0,0)$ to $M = (\pm1,\mp1)$, in conjunction with the above findings, the binding can be rather clearly represented by the following vbL icon
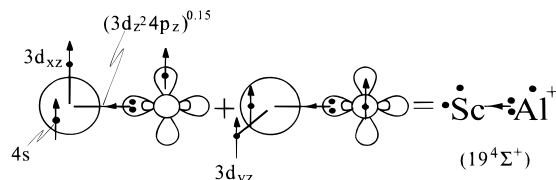
$$(18\,^4\Sigma^-)$$

This picture indicates a hybrid $(3d_{z^2}4s4p_z)^{1.20}$ σ orbital, two half π bonds and a σ harpooning bond from Al to Sc⁺; via the π and σ frames 0.12 and 0.20 e⁻ are transferred from Al to Sc⁺, respectively.

$15\,^4\Sigma^+$, $19\,^4\Sigma^+$. The dominant CAS equilibrium configurations of these states are $|15\,^4\Sigma^+\rangle \sim 0.97|1\sigma^2 2\sigma^1 3\sigma^1 1\delta_\sigma^1\rangle$ and $|19\,^4\Sigma^+\rangle \sim 0.67(|1\sigma^2 2\sigma^1 1\pi_x^1 2\pi_x^1\rangle + |1\sigma^2 2\sigma^1 1\pi_y^1 2\pi_y^1\rangle)$. The two states interact through an avoided crossing, appearing as a small shoulder in the repulsive part (~5.9 bohr) in the $15\,^4\Sigma^+$ PEC. In this state the bonding is caused by a half σ bond, while in the $19\,^4\Sigma^+$ the bonding is due to a dative bond from Al to Sc⁺ at $R_e = 3.820$ and 3.332 Å and $D_e = 13.0$ and 7.8 kcal/mol for the $15\,^4\Sigma^+$ and $19\,^4\Sigma^+$ states, respectively, with respect to Sc⁺-(^{3}D; $M = 0, \pm1$) + Al(^{2}P; $M = 0, \mp1$) atoms. Last, it is interesting that at the SCF level the binding energy of the $15\,^4\Sigma^+$ is 11 kcal/mol, almost equal to its MRCI value.
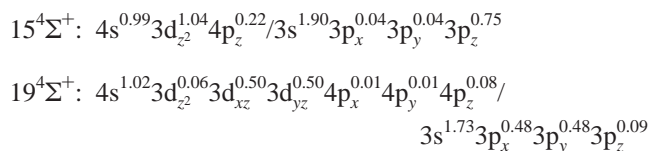
The following vbL icons explicate the bonding character,

$$(15\,^4\Sigma^+)$$

The Mulliken population analysis at the minima of the two

$$(19\,^4\Sigma^+)$$

states are

$15^4\Sigma^+$: $4s^{0.99}3d_{z^2}^{1.04}4p_z^{0.22}/3s^{1.90}3p_x^{0.04}3p_y^{0.04}3p_z^{0.75}$

$19^4\Sigma^+$: $4s^{1.02}3d_{z^2}^{0.06}3d_{xz}^{0.50}3d_{yz}^{0.50}4p_x^{0.01}4p_y^{0.01}4p_z^{0.08}/$
$$3s^{1.73}3p_x^{0.48}3p_y^{0.48}3p_z^{0.09}$$

Overall about 0.2 e$^-$ migrates from Al to Sc$^+$ in both states.

Comparing the $6^4\Delta$ and the $15^4\Sigma^+$ states, we see that the only difference is the orbital where the d electron on Sc$^+$ (d$_\delta$ and d$_\sigma$, respectively) is localized. Although this electron does not participate in the bonding process of either state, the $6^4\Delta$ has a shorter bond distance by 0.433 Å and about twice as high binding energy. The obvious reason is that in the case of the Δ state the Al p$_z$ electron is transferred to the hybridized $3d_{z^2}4p_z$ orbital of Sc$^+$, while in the case of Σ symmetry the only allowed process is a promotion af about 0.2 e$^-$ to the 4p$_z$ orbital of Sc$^+$ from the 3p$_z$ Al function.

5. Final Remarks

By employing the MRCI (CASSCF+1+2) methodology coupled with the ANO/cc-pVTZ = [(7s6p4d3f)$_{Sc}$(5s4p2d1f)$_{Al}$] basis, we have explored the electronic structure of the diatomic species scandium aluminide cation, ScAl$^+$. To the best of our knowledge, no experimental or theoretical results exist in the literature. We report absolute energies, bond lengths, binding energies, harmonic frequencies, Mulliken charges, electronic energy gaps, and potential energy curves for a total of 21 states. Our main findings can be synopsized as follows:

1. Due to the relatively small ionization potential difference of Sc and Al atoms [0.58 eV (experiment), 0.41 eV (theory)] the first three states, X$^2\Delta$, 1$^2\Pi$, and 2$^2\Sigma^+$ correlate to Sc(^{2}D) + Al$^+$(^{1}S) while the rest of the states dissociate to Sc$^+$ + Al(^{2}P).

2. Formally, we have characterized the ground state as X$^2\Delta$ at the MRCI level of theory. However, we would like to emphasize that the energy difference between the 1$^2\Pi$ and X$^2\Delta$ states is a mere 0.6 kcal/mol at the MRCI level; by using the multireference Davidson correction the order is reversed, the 1$^2\Pi$ becoming the ground state by 0.3 kcal/mol. An additional correction with respect to the zero point energy does not further affect the ordering because both states have practically the same $\omega_e \approx 165$ cm^{-1}. Therefore, it is obvious that within the accuracy of our calculations these two states should be considered as degenerate. For the next state of $^2\Sigma^+$ symmetry, we feel more confident of its being the second excited state with a T_e of about 1 kcal/mol in both the MRCI and MRCI+Q levels.

3. With the exception of four states, namely, 17$^4\Pi$, 18$^4\Sigma^-$, 19$^4\Sigma^+$, and 20$^2\Sigma^-$ (CASSCF only), which are unbound with respect to Sc + Al$^+$ (by 0.2, 0.7, and 2.7 kcal/mol at MRCI level, respectively, for the three first states), the rest of the states are bound with respect to these end products.

4. The binding energies and equilibrium bond lengths vary from 7.8 (19$^4\Sigma^+$) to 32.6 (3$^4\Sigma^-$) kcal/mol and 2.533 (18$^4\Sigma^-$) to 3.820 (15$^4\Sigma^+$) Å at the MRCI level. The corresponding numbers at the MRCI+Q level are 9$-$34 kcal/mol and 2.56$-$3.75 Å.

5. The bonding of the ScAl$^+$ system is analyzed in essence at the CASSCF level with the help of the Mulliken population analysis, the dominant configurations of the reference space and visualized by valence bond Lewis icons. The bonding character ranges from a half σ bond to a whole σ + two half π bonds.

6. With the exception of the ground and the first two excited states where 0.5 e$^-$ is transferred from Sc to Al$^+$, in the rest of the states charge migrates from Al to Sc$^+$ varying from 0.2 to 0.5 e$^-$.

7. On account of avoided crossings three of the states, i.e., 8$^2\Delta$, 16$^4\Delta$, and 18$^4\Sigma^-$, present two minima, a local and a global.

8. The harmonic frequencies (ω_e) range from a minimum value of 90 (15$^4\Sigma^+$) to a maximum of 325 cm^{-1} (18$^4\Sigma^-$), thus reducing the corresponding binding energies by 0.13$-$0.46 kcal/mol.

9. Figure 2 shows an energy level diagram of all computed states in ascending energy order. For reasons of comparison the diagram of isovalent species ScB$^+$ (ref 6a) is also included, with single lines connecting "similar" states.

10. It is rather clear from Figure 2 that for states differing by about 1 mhartree we cannot be sure for their relative order, even within the nonrelativistic Hamiltonian ansatz employed in the present study. Disregarding the first three states (X$^2\Delta$, 1$^2\Pi$, 2$^2\Sigma^+$), the following pairs differ by about 1 mhartee: (5$^4\Phi$, 6$^4\Delta$), (7$^2\Sigma^-$, 8$^2\Delta$), (9$^2\Pi$, 10$^4\Pi$), (12$^2\Phi$, 13$^2\Pi$), (14$^2\Delta$, 15$^4\Sigma^+$), (16$^4\Delta$, 17$^4\Pi$), and (17$^4\Pi$, 18$^4\Sigma^-$). Notice that for the pair of "degenerate" states 14$^2\Delta$, 15$^4\Sigma^+$, the ordering is reversed by adding the zero point energy correction $\Delta\omega_e/2 = (284 - 90)/2 = 97$ cm^{-1} = 0.3 kcal/mol. No other pair of quasi-degenerate states is influenced due to zero point energy differences; in addition, the given ordering is maintained after applying the Davidson +Q correction.

References and Notes

(1) Zou, J.; Fu, C. L. *Phys. Rev. B* **1995**, *51*, 2115.
(2) Behm, J. M.; Morse, M. D. *Proc. SPIE-Int. Soc. Opt. Eng.* **1994**, *2124*, 389.
(3) Sokolovskaya, E. M.; Kazokova, E. F.; Podd'yakova, E. I. *Metalloved. Term. Obrab. Met.* **1989**, *11*, 29.
(4) Pygai, I. N.; Vakhobov, A. V. *Izv. Akad. Nauk, SSSR Met* **1990**, *5*, 55.
(5) Meschel, S. V.; Kleppa, O. J. *NATO ASI Ser., Ser. E* **1994**, *256*, 103.
(6) (a) Kalemos, A.; Mavridis, A. *Adv. Quantum Chem.*, **1998**, *32*, 69. (b) Kalemos, A.; Mavridis, A. *J. Phys. Chem. A* **1998**, *102*, 5982. (c) Kalemos, A.; Mavridis, A. *J. Phys. Chem. A* **1999**, *103*, 3336. (d) Kalemos, A.; Mavridis, A. Submitted for publication.
(7) Moore, C. E. *Atomic Energy Levels*; NSRDS-NBS Circular No. 35; Washington, DC, 1971.
(8) Bauschlicher, C. W., Jr. *Theor. Chim. Acta* **1995**, *92*, 183.
(9) Dunning, T. H., Jr. *J. Chem. Phys.* **1989**, *90*, 1007. Kendall, R. A.; Dunning, T. H., Jr.; Harrison, R. J. *J. Chem. Phys.* **1992**, *96*, 6796.
(10) Werner, H.-J.; Knowles, P. J. *J. Chem. Phys.* **1988**, *89*, 5803. Knowles P. J.; Werner, H.-J. *Chem. Phys. Lett.* **1988**, *145*, 514. Werner, H.-J.; Reinsch, E. A. *J. Chem. Phys.* **1982**, *76*, 3144. Werner, H.-J. *Adv. Chem. Phys.* **1987**, *LXIX*, 1.
(11) Docken, K.; Hinze, J. *J. Chem. Phys.* **1972**, *57*, 4928.
(12) Werner, H.-J.; Meyer, W. *J. Chem. Phys.* **1981**, *74*, 5794.
(13) MOLPRO 96 is a package of ab initio programs written by Werner, H.-J.; Knowles, P. J. with contributions by Almlof, J.; Amos, R. D.; Berning, A.; Deegan, M. J. O.; Eckert, F.; Elbert, S. T.; Hampel, C.; Lindh, R.; Meyer, W.; Nicklass, A.; Peterson, K.; Pitzer, R.; Stone, A. J.; Taylor, P. R.; Mura, M. E.; Pulay, P.; Schuetz, M.; Stoll, H.; Thorsteinsson, T.; Cooper, D. L.
(14) Shepard, R.; Shavitt, I.; Pitzer, R. M.; Comeau, D. C.; Pepper, M.; Lischka, H.; Szalay, P. G.; Ahlrichs, R.; Brown F. B.; Zhao, J.-G. *Int. J. Quantum Chem.* **1988**, *S22*, 149.
(15) Botch, B. H.; Dunning, T. H., Jr.; Harrison, J. F. *J. Chem. Phys.* **1981**, *75*, 3466.
(16) (a) Langhoff, S. R.; Davidson, E. R. *Int. J. Quantum Chem.* **1974**, *8*, 61. (b) Blomberg, M. R. A.; Sieghbahm, P. E. M. *J. Chem. Phys.* **1983**, *78*, 5682.
(17) Emsley, J. *The Elements*; Clarendon Press: Oxford, 1991.